# Feasibility of multi-physics reservoir monitoring for heavy oil

H. Passalacqua, S. Davydycheva, & K. Strack,

2018

Heavy Oil, Heavy Oil Conference Kuwait,
SPE-193690-MS

SPE-193690-MS

# Feasibility of multi-physics reservoir monitoring for heavy oil

H. Passalacqua, Australian College of Kuwait, Kuwait
S. Davydycheva, KMS Technologies, Houston, Texas
K. Strack, KMS Technologies, Houston, Texas

This paper was prepared for presentation at the SPE International Heavy Oil Conference and Exhibition held in Kuwait, 2018.

## Abstract

A new microseismic-electromagnetic (EM) acquisition system for reservoir monitoring includes surface and borehole hardware, processing software and interpretation methodology. For heavy oil reservoirs it allows mapping of steam/water flood fronts and surveillance of cap-rock integrity. The new array acquisition architecture combines novel technologies which reduces operational cost, due to unlimited channels capability: EM and microseismic acquisition is in the same receiver node to optimize the synergy between the methods.

While microseismic channels address seal integrity information, EM data are used to track fluids, due to their high sensitivity to the fluid resistivity. The fluid resistivity drops strongly with mobility increase and pore size variation. Dense data further reduce the cost per receiver in a surface location. EM channels provide three-component (3C) electric and 3C magnetic data acquired on the surface and in shallow vertical boreholes. For later versions and deeper reservoirs deep wireline receiver with through casing measurement capabilities are planned. We include in the system an independent physics verification measurement using a differential approach to the surface data called focused source EM (FSEM) with practically little cost.

Carrying out feasibility for each reservoir is key to control risk and cost. The feasibility includes 3D EM modeling, which allows integrating typically complex nature of the reservoir, and on-site EM noise test to tie 3D modeling to actual measured voltages.

3D modeling feasibility for a heavy oil reservoir proves the methodology to monitor the boundaries of the steam flood with accuracy and with high fidelity. Above the edges of the flooded (higher-temperature – lower-resistivity) area the results predict time-lapse EM anomaly exceeding 500%.

The entire system is coupled with processing and 3D modeling/inversion software, significantly

streamlining the workflow for the different methods.

The system is capable of measuring and integrating the 3C of the electric field and 3C of the magnetic field in order to map the steam front and at the same time measuring microseismic occurrences in order to monitor seal stability. Channels capability of the system is practically unlimited allowing a denser coverage of the area in order to increase resolution and improve inversion.

## Introduction

The present paper further develops multi-physics methodology suggested by Passalaqua et al. (2016) for monitoring of steam-flooded heavy oil reservoirs. Here we concentrate on EM monitoring feasibility, while the system and the methodology include multi-channel data acquisition with microseismic and EM sensors (Figure 1). Microseismic sensors monitor the seal integrity due to possible reservoir leakage in the upper layer (Carlson, 2013), while EM sensors provide unique opportunities to track fluid movements and flow boundaries due to differences in the fluid resistivity.

*Figure 1- Field equipment and hardware components. Orange boxes: 195-channel microseismic-EM receivers KMS-820.*

The multi-physics measurements are based on the fact that the steam injection increases the original pressure of the reservoir producing small fractures that in turn generate seismicity and decrease the resistivity of the fluids. Both effects are measurable by the sensors measuring seismic and electrical properties of the subsurface. The measurements are made in 4D, repeating the same according to time periods dictated by the reservoir simulation.

## Methodology

The hardware system (Figure 2) has been developed using state-of-the art seismic architecture with wireless array and large memory SD cards. EM and seismic sensors are connected to the same node. Some of the characteristics of our system are:

- Broad band (DC-80 kHz, low noise, low drift)

- Multi-components, multi-physics (microseismic and electromagnetic)
- Transition to digital sensors
- High dynamic range
- 8 km long range wireless, WIFI (2 types) and noise free internet streaming
- Autonomous, can record for weeks
- GPS timing & atomic crystal (marine option)
- Lower cost

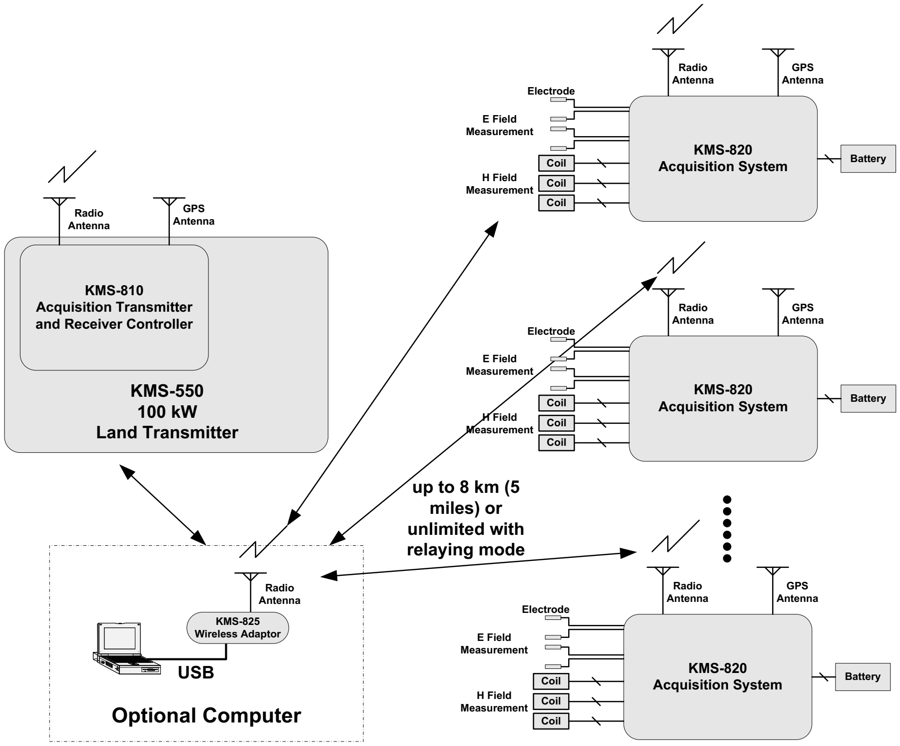

*Figure 2 – The hardware system*

Transmitters' synchronization and current stability better than 0.5% for periods of days are necessary requirements to use better arrays to increase the spatial resolution. Large oversampling, dynamic range, long term stability with time and temperature are also key for monitoring applications. Very stable pre-amplifiers are used to avoid effects due to the heat from sun light (Rüter and Strack 1995; Jiang et al. 2015).

The cornerstone of our methodology is the combination of seismic data with full EM field measurements. We developed a commercial land microseismic-EM system for reservoir monitoring. The system includes three-component (3C) electrical and magnetic receivers situated on the Earth surface and in shallow vertical boreholes, to allow for vertical electric field measurement, for which we use a commercial shallow borehole tool (SBHT, Figure 3). Shallow vertical observation boreholes of the depth from 20 to 50 m can easily be prepared. The ground is exited by grounded horizontal dipole transmitter.

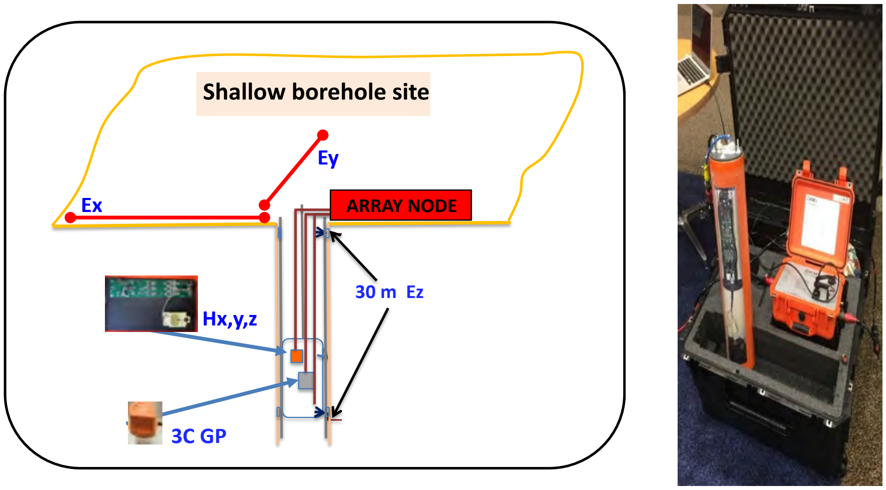

*Figure 3: Shallow borehole tool overview.*

Both magnetic and electric field are measured as one portion of the reservoir tends to be conductive (flooded area) and the other part will be resistive (hydrocarbon saturated) (Colombo et al. 2010, Strack et al. 1989).

Every monitoring project starts with a 3D modeling feasibility study, and finishes with data interpretation. For the both feasibility modeling and the interpretation it is critically important to have accurate data on the background formation resistivity coming from available resistivity logs taken from vertical or any other available wells and from any other a priory information. While constructing such a background model, taking the resistivity anisotropy into account is a must. Anisotropy in electrical resistivity is key for understanding EM data and for correct geological interpretation. In general, most sedimentary rocks are electrically anisotropic (Figure 4) due to sand-shale laminations. Shale-sand laminations usually exhibit vertical resitivities (Rv) higher than horizontal resistivities (Rh) (Yu et al. 2001; Barber et al. 2004). Current tends to flow easier in the horizontal direction along shales in tha case of laminated shale-sand sediments. The vertical resistivity will be higher and influenced by oil saturated sands. Logs in Figure 5 show examples of this. EM measurements are strongly affected by electrical anisotropy as the current flow tends to be in both directions, horizontal and vertical. This is why is critical the consideration of anisotropy. The measurement of both vertical and horizontal components of the electromagnetic field is essential. Shale formations tend to be very anisotropic, with Rv to Rh ratio reaching 10, but even in conventional formation Rv/Rh is in the range of 1.5-2. The presence of hydrocarbons in these rocks will generate high resistivity anomalies (Passalacqua 1983; Eadie 1980). The magnitude of these anomalies depends on the anisotropy.

New logging tools capable of tensor resistivity measurements recently developed have allowed the possibility of improving the EM interpretation offering the possibility of linking both sets of data for a more realistic interpretation of EM data.

In Figure 5 we show two examples of triaxial induction logging. In both cases the vertical resitivity is higher than the horizontal resistivity. These tools allow a better calibration of the EM multicomponent measurements. When the modern anisotropy logs are unavailable, the anisotropy can be estimated from conventional resistivity logs using well-known equivalence principle (Keller & Frischknecht, 1967).

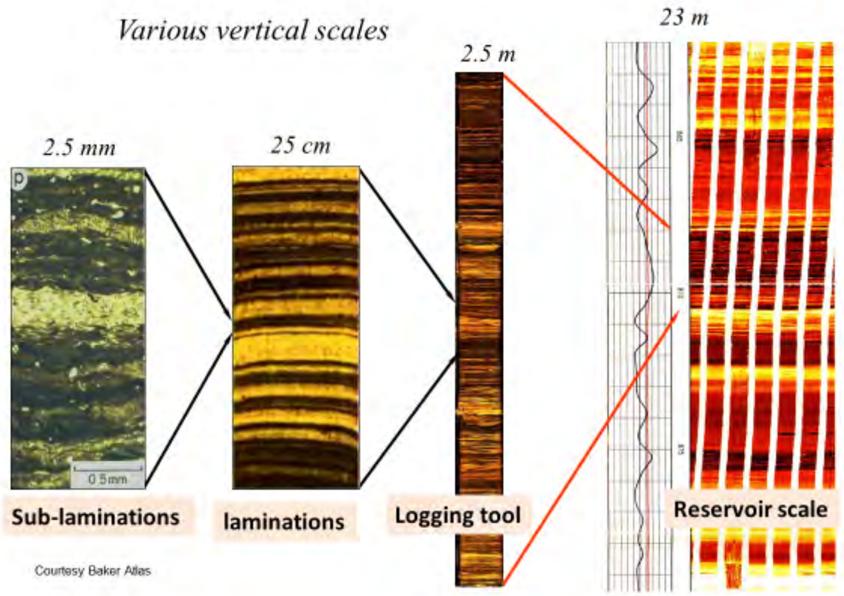

*Figure 4 – Layering of sand-shale sequences shown in three different scales by resistivity image logs. From left to right: Electron microscope image, image at lamination scale (1 inch to 1 centimeter) derived from core samples, resistivity image log (1 track) from a wireline logging tool, and at far right a typical image log section from a 6-arms resistivity imager.*

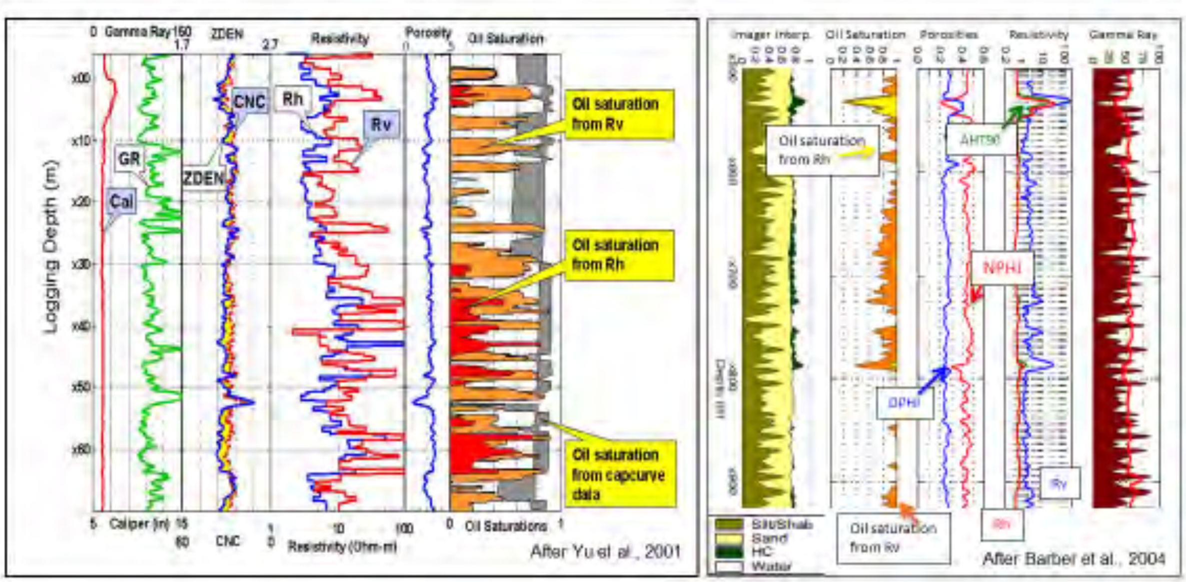

*Figure 5 – In this figure we show two triaxial induction log interpretations from two contractors (Yu et al. 2001; Barber et al. 2004). GR is Gamma Ray log, CNC and ZDEN are neutron and density logs, respectively, AHT90 is a deep induction log. In both cases the vertical resistivity*

*(Rv) shows higher oil saturation than in the horizontal resistivity (Rh). The Rv is more sensitive to the thin laminated shale sequence.*

The data are calibrated using available well logs and linked to microseismic data. Calibrating available borehole data against surface EM measurements gives greater sensitivity to fluid variations in the pore space. A 3D modeling-based feasibility study is performed for each application. Those EM components that exhibit the strongest anomalies, determined by modeling, are combined with on-site noise measurements to establish technical and commercial viability and to define survey and operational parameters.

A high level workflow for the processing and interpretation of EM and microseismic data is shown in Figure 6. Both kinds of data are separated at the common node in order to perform data specific filtering. The data is then inverted and images are generated, and finally a unified interpretation is produced.

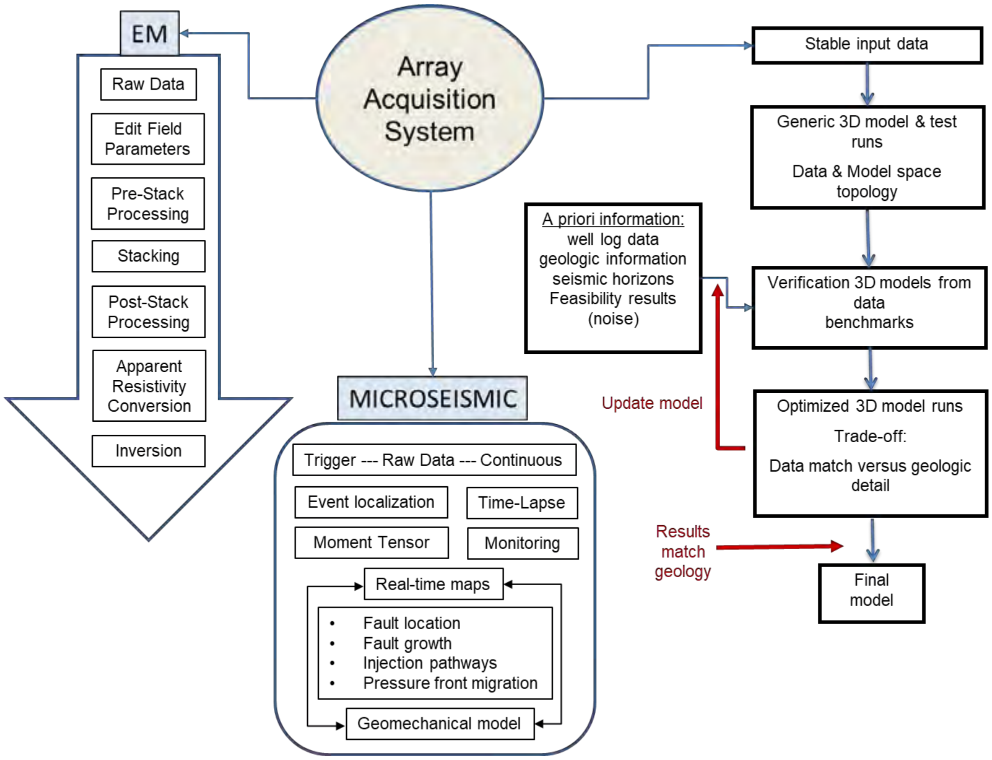

*Figure 6 - Data processing workflow for controlled source EM and microseismic.*

Figure 7 shows in more detail the processing workflow for the EM data. From left to right and top to bottom it starts with the raw data, these are filtered and stacked to produce the electric (top) and magnetic fields (bottom). On the right stacks are filtered from noise. Finally, at the bottom we show the inversion results using smoothness constrained inversion, and the 3D rendering of the interpretation.

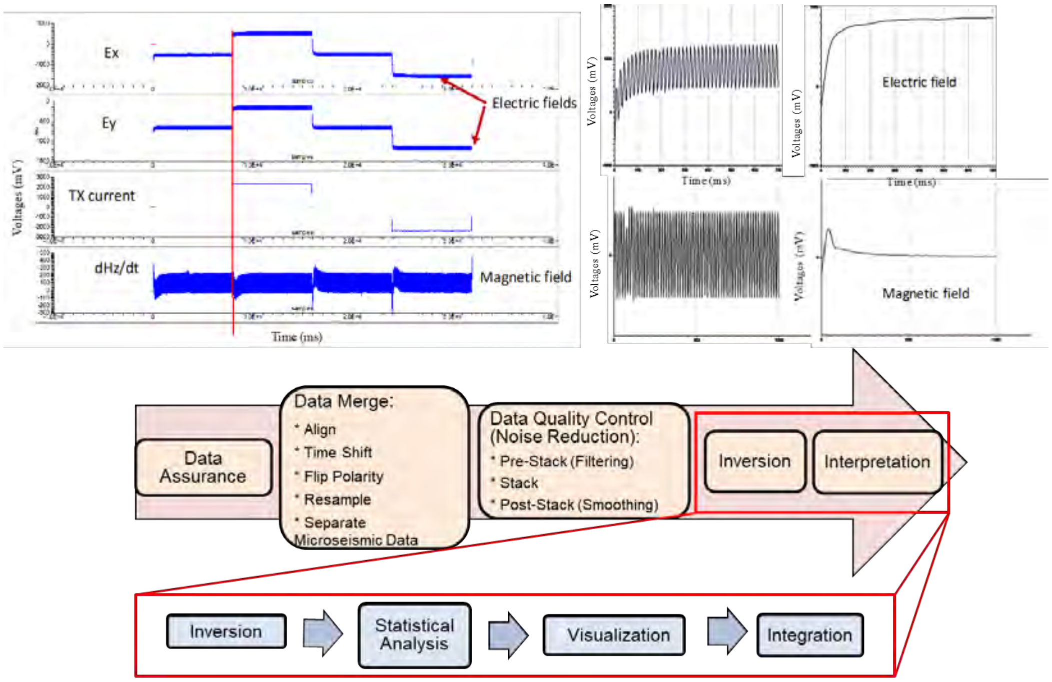

*Figure 7 - Processing workflow for EM data.*

Figure 8 shows vertical cross-section of a heavy oil reservoir (Passalaqua et al. 2016). The reservoir overburden includes clastic water-saturated material, the bottom of which has elevated salinity which reflects in a reduced (2 Ωm) resistivity. The underlying heavy oil reservoir has the resistivity of ~4 Ωm (depicted in green). The free water zone having the resistivity of ~1.5 Ωm is below the heavy oil reservoir. We try to map steam-flooded section of the reservoir, which has reduced resistivity due to its higher temperature. Its approximate 3D model (in the bottom) is used for 3D modeling feasibility study. The blue parallelepiped represents the steam flooded area of 500x500x140 m.

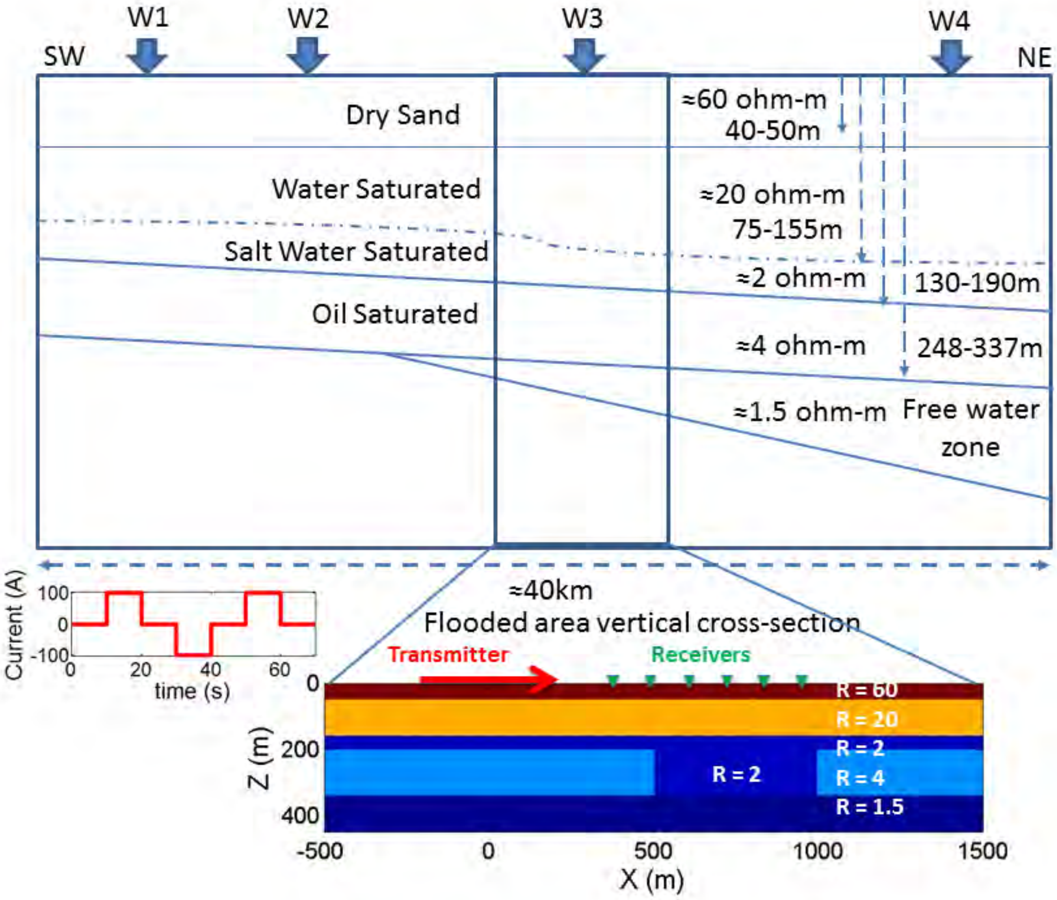

*Figure 8 - Geologic section of a heavy oil reservoir (top) and its simplified 3D resistivity survey model used for 3D modeling feasibility study (bottom).*

A grounded horizontal electric 400-m long dipole transmitter situated at the origin excites the formation with rectangular impulses (square waves) of 100 A, with pauses between them. As the steam front moves, the multicomponent EM receivers above the flood area on the surface (shown as triangles) records the respective time-lapse response. The *x*-directed dipole transmitter is co-aligned with the waterfront propagation direction, for simplicity of the analysis. In-line receivers were chosen, as they give the strongest response to the resistive reservoir (Strack, 1992). To estimate the sensitivity to the reservoir resistivity the response of all three components of the magnetic and the electric field, including the vertical component E*z* were simulated at several times after the transmitter current turn-off.

Synthetic responses of the offset-corrected horizontal electric field component E*x* are shown in Figure 9 as a function of the distance to the transmitter, with the relative changes (bottom), i.e. measurements compared to a fully oil saturated state. On the left we show the isotropic case as on the model depicted in Figure 8. On the right we added a moderate anisotropy in oil-saturated rocks only, with the vertical resistivity Rv = 8 ohm-m and the horizontal resistivity Rh = 4 ohm-m (as it was in the isotropic case). The difference is visible, especially at early times.

The vertical (E*z*) electric field components are shown in Figure 10 (they are not offset corrected) as a function of time after the transmitter turn-off (top) and relative responses as a function of the distance (bottom). E*z* is the most sensitive to vertical currents significantly affected by resistive/conductive (unflooded/flooded) rocks. This component demonstrates very high sensitivity to the reservoir properties: late-time responses are significantly affected, especially above the flood area edges at 500 and 1000 m. Thus, the flooded area contour may be determined with great accuracy through the measurement of E*z* component using SBHT in vertical boreholes above the reservoir. Since the reservoir is relatively shallow, the effect is strong enough at relatively early times below 1 s. Note that time-domain EM measurements do not require large offsets typically needed for frequency-domain methods. E*z* sensitivity reveals itself at late times after turn-off, where deeper lying strata respond. They are noticeably affected by the anisotropy in oil-saturated rocks (on the right). The signal level was well above the typical noise floor measured on the site for each feasibility study.

Figure 11 demonstrates magnetic field response (magnetic induction dB*z*/dt). It is in the range of several per cent and not much affected by the anisotropy. Note that the traditional inline dipole-dipole measurement E*x* shows reduction of the signal level above the more conductive flooded zone, since the electric field is more sensitive to resistors, while the magnetic response, on the contrary, shows some elevation above the flooded zone, being more sensitive to conductors. E*x* response is much smaller than Ez response, since Ex is mostly sensitive to horizontal currents, much less affected by relatively thin resistors (reservoir), while E*z* is much affected by thin horizontal resistors.

We do not show other components, E*y*, dB*x*/dt and dB*z*/dt, since they are identically equal to zero due to the model symmetry with respect to (*x,z*)-plane in our simplified feasibility study.

The EM responses were simulated using a 3D finite-difference method by Davydycheva & Druskin (1999) which allows for arbitrary resistivity anisotropy.

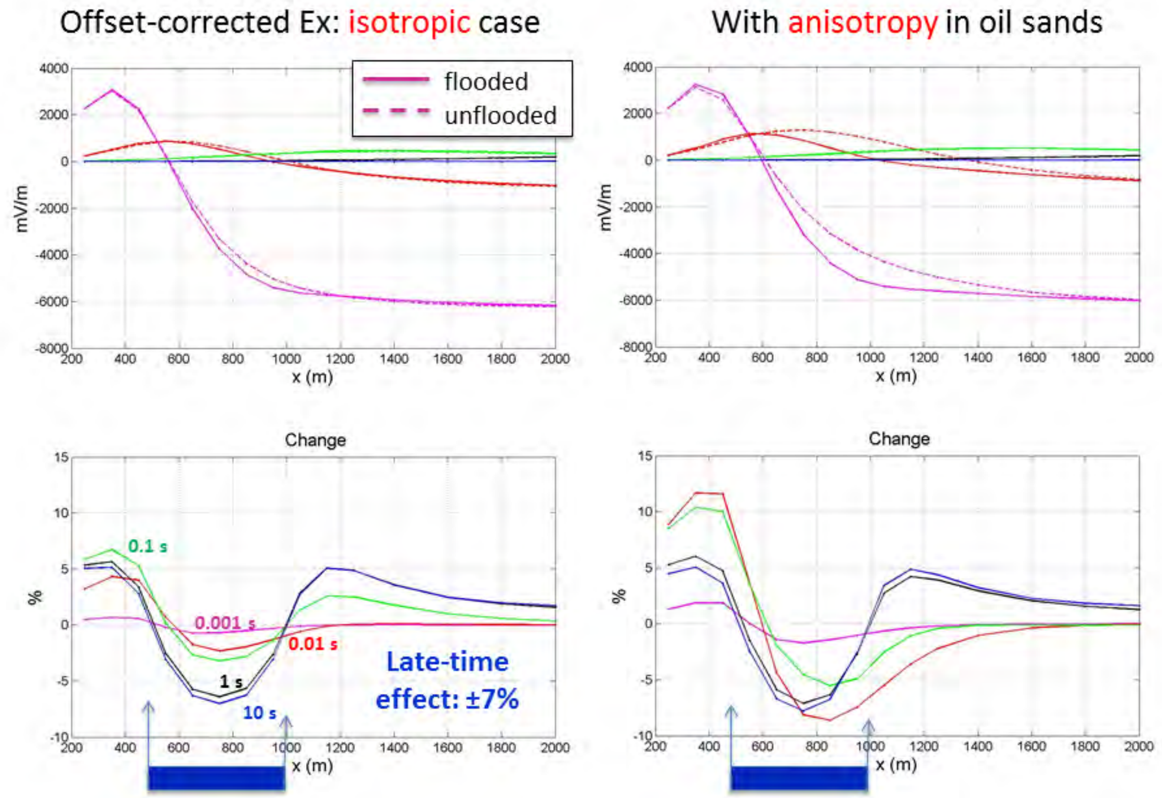

*Figure 9 - Inline electric field (Ex-Ex) response, as a function of the distance to the transmitter, on the left: isotropic case, on the right: anisotropy added in oil-saturated rocks*

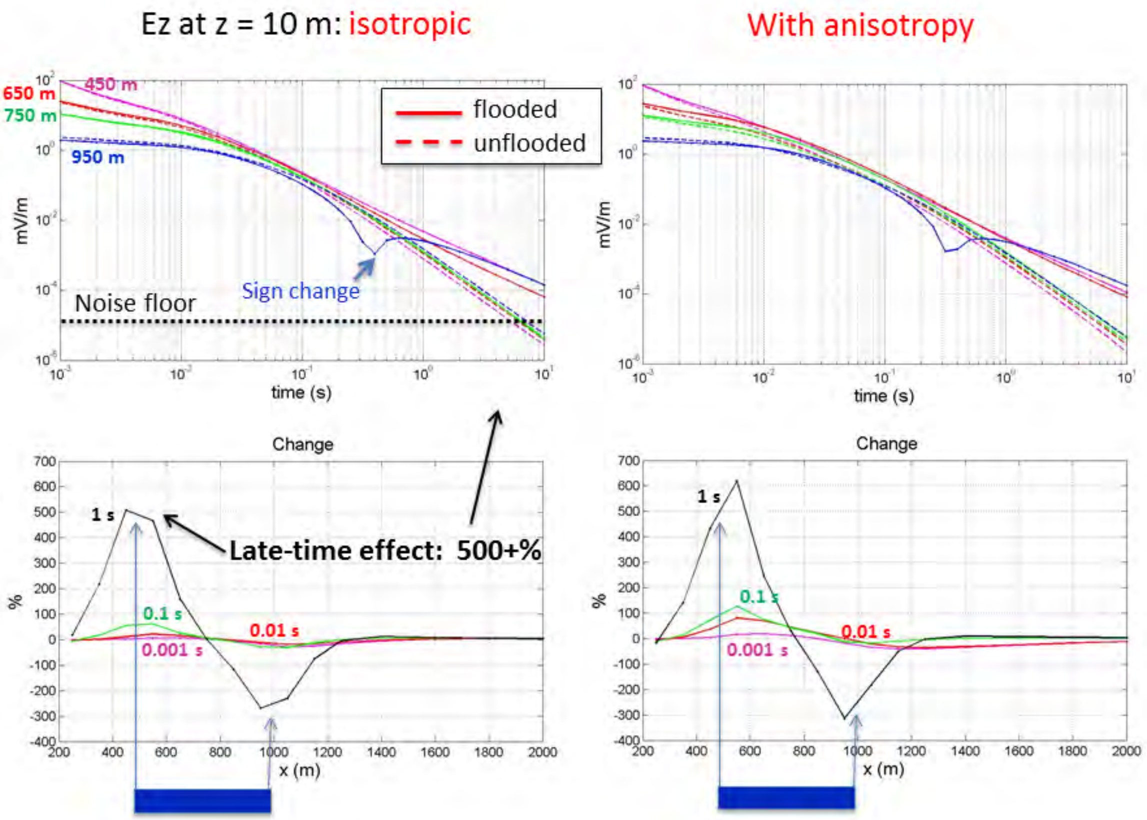

*Figure 10 - Vertical electric field response (Ex-Ez) as a function of time after turn-off (top), with the percentage change shown as a function of the distance to the transmitter (bottom).*

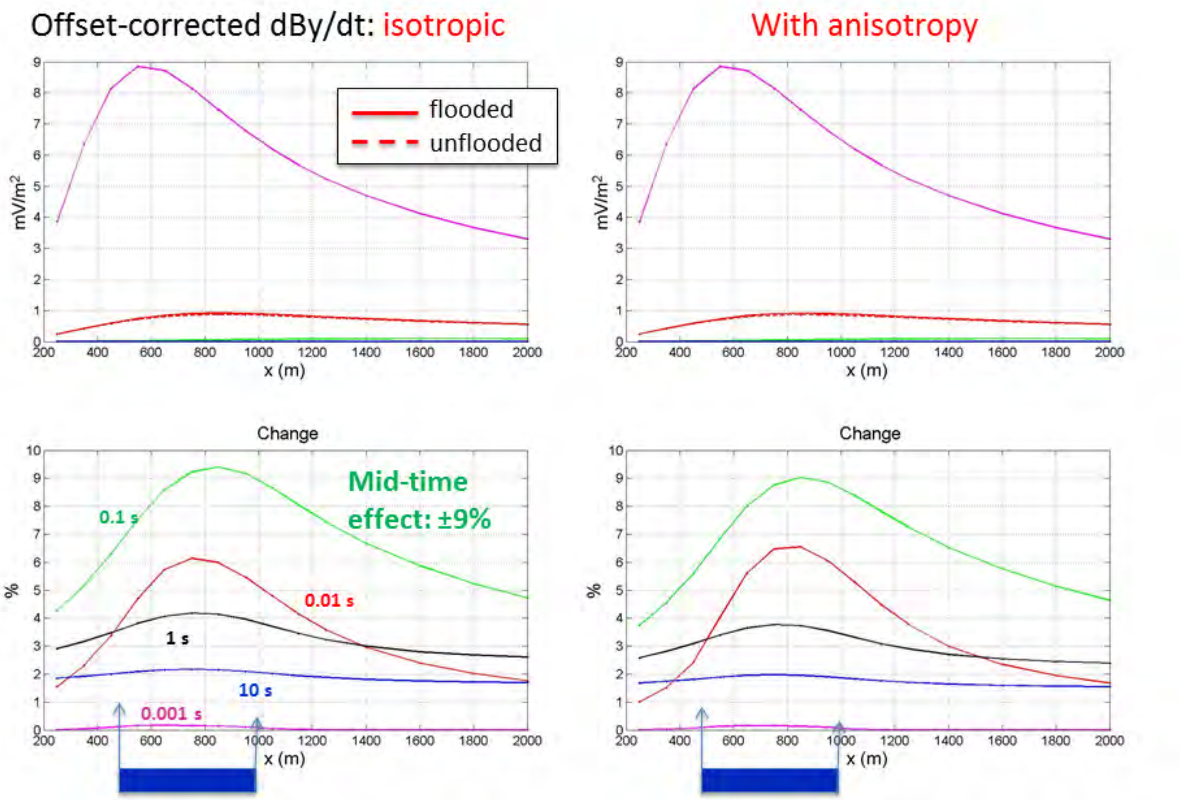

*Figure 11 – Magnetic field/induction response, as a function of the distance to the transmitter.*

Measurement of the vertical electric field requires drilling shallow vertical wells to place the receivers. If those are unavailable, an alternative focused-source EM (FSEM) measurement by Davydycheva and Rykhlinski (2011) and Davydycheva (2018) can help. The FSEM configuration works similar to focused borehole laterologs and provides high sensitivity to thin horizontal resistors. The differences between adjacent receivers is subtracted and approriately normalized to only produce a sensitivity to ~~the~~ the vertical electric field.

We have run field tests with the both dipole-dipole measurements and FSEM over a salt dome to verify the methodology and the system functionality (see Paembonan et al. 2018).

## Conclusions

The multi-physics measurements offer the great advantage of monitoring two critical aspects of the production of heavy oil fields subject to steam injection processes, such as the integrity of the reservoir seal and the progress of the steam front. Our instrumentation allows simultaneous microseismic and multi-component EM measurements (3C electric and 3C magnetic data), and feasibility modeling in 3D determines which of those components best respond to changes in electrical properties of a particular reservoir.

Many feasibility studies for a variety of reservoir have been carried out. Heavy oil reservoir appears to be one of the most promising applications. We have also started a pilot field installation which is ongoing.

## Acknowledgments

We appreciate the support of Tilman Hanstein and Xiayu Xu by carrying the noise tests and collecting field data. We also acknowledge the trust received over the years from many companies. They include: Aramco, BP, ENI, Ormat, PTTEP, Shell, and WellDynamics. We also thank KMS Technologies and Australian college of Kuwait (ACK) for permitting to publish this paper.

## References

Barber, T., Anderson, B., Abubakar, A., Broussard, T., Chen K.-C., Davydycheva S., Druskin V., Habashy, T.M., Homan, D.M., Minerbo, G., Rosthal, R., Schlein, R., and Wang, H., 2004, Determining formation resistivity anisotropy in the presence of invasion, Society of Petroleum Engineers, Annual Technical Conference, Paper 90526.

Carlson, M., 2013, Caprock failure at Joslyn, Journal of Canadian Heavy Oil Ass., presented at the SPE Heavy Oil Conference held in Calgary, Alberta, Canada 12-14th June 2012.

Colombo, D., Dasgupta, S., Strack, K.-M., and Yu, G., 2010, Feasibility study of surface-to-borehole CSEM for oil-water fluid substitution in Ghawar field, Saudi Arabia, AAPG GEO 2010 Middle East: Innovative Geoscience Solutions – Meeting Hydrocarbon Demand in Changing Times, Manama, Bahrain.

Davydycheva, S., 2018, Method and apparatus for detecting and mapping subsurface anomalies, U.S. Patent 9891339 B2.

Davydycheva, S., and Rykhlinski, N., 2011, Focused Source electromagnetic survey versus standard CSEM: 3D modeling in complex geometries, Geophysics, 76, 1, F27-F41.

Davydycheva, S., and Druskin, V., 1999, Staggered grid for Maxwell's equations in arbitrary 3-D inhomogeneous anisotropic media, in: Oristaglio, M., and Spies, B., Eds. *Three-dimensional electromagnetics*: SEG, 119-137.

Eadie, T., 1980, Detection of hydrocarbon accumulations by surface electrical methods - feasibility study, M. S. Thesis, University of Toronto.

Eidesmo, T., Ellingsrud, S., MacGregor, L.M., Constable, S., Sinha, M.C., Johansen, S., Kong, F.N., and Westerdahl, H., 2002, Sea Bed Logging (SBL), a new method for remote and direct identification of hydrocarbon filled layers in deep water areas, First Break, 20, 144-152.

He, Z., Hu, W., and Dong, W., 2010, Petroleum Electromagnetic Prospecting Advances and Case Studies in China, Surveys in Geophysics, 31, 207-224.

He, Z., Liu, X., Weiting, W., and Zhou, H., 2006, Mapping reservoir boundary by borehole-surface TFEM: Two case studies, The Leading Edge, 24, 896-900.

Jiang, J., Aziz, A.A., Liu, Y., and Strack. K.-M., 2015, Geophysical acquisition system, US 9,057,801.

Keller, G.V., and Frischknecht, F.C., 1967, Electrical methods in geophysical prospecting, Pergamon Press.

Kumar, D., and Hoversten, G.M., 2012, Geophysical model response in a shale gas, Geohorizons, Journal of Society of Petroleum Geophysicists, India, 16, 31-37.

Neese, J.W. and Thomsen, L., 2014, Seismic processing of numerical EM data, SEG

Passalacqua, H., and Strack, K.-M., 2016, Integrated geophysical reservoir monitoring for heavy oil, SPE-184089-MS.

Passalacqua, H., 1983, Electromagnetic fields due to a thin resistive layer, Geophysical Prospecting, 31, 945-976.

Paembonan, A.Y., Arjwech, R., Davydycheva, S., Hanstein, T., Smirnov, M., Strack, K.-M., 2018, 1D and 3D interpretations to confirm the salt dome profile, 24th EM Induction Workshop, Helsingør, Denmark, August 12-19, 2018.

Rüter, H., and Strack, K.-M., 1995, Method of processing transient electromagnetic measurements in geophysical analysis, US patent 5,467,018.

Strack, K.-M., and Aziz, A.A., 2013, Advances in electromagnetics for reservoir monitoring, Geohorizons, 32-44, (Special shale issue).

Strack, K.-M., 2004, Surface and borehole integrated electromagnetic apparatus to determine reservoir fluid properties, US 06739165.

Strack, K.-M., 2003, Integrated borehole system for reservoir detection and monitoring, US 06541975 & US 06670813.

Strack, K.M., and K. Vozoff, 1996, Integrating long-offset transient electromagnetics (LOTEM) with seismics in an exploration environment, Geophysical Prospecting, 44, 99-101.

Strack, K.-M., 1992, Exploration with deep transient electromagnetics, Elsevier.

Strack, K.-M., Lebrocq, K., Moss, D. C., Petry, H., Vozoff, K. and Wolfgram, P. A., 1989, Case histories of long-offset transient electro-magnetics (LOTEM) in hydrocarbon exploration, First Break 7, 467-477.

Thomsen, L., 2014, Electromagnetics and seismics: The deep connection, SEG Technical

Program Expanded Abstracts, 855-859.

Tietze, K., Ritter, O., and Veeken, P., 2015, Controlled-source electromagnetic monitoring for reservoir oil saturation using a novel borehole-to-surface configuration, Geophysical prospecting, 63, 1-23.

Yu. L., Fanini. O. N., Kriegshäuser. B. F., Koelman. J.M.V. and van Popta. J., 2001, Enhanced evaluation of low-resistivity reservoirs using new multicomponent induction log data, Petrophysics, 42, 611-623.

KMS Technologies – KJT Enterprises Inc.
11999 Katy Freeway, Suite 160
Houston, Texas 77079
USA

info@KMSTechnologies.com

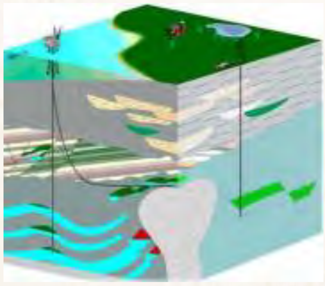

**www.KMSTechnologies.com**